Water Resources and Industry 28 (2022) 100186

Contents lists available at ScienceDirect

Water Resources and Industry

journal homepage: www.elsevier.com/locate/wri

Removal of nonsteroidal anti-inflammatory drugs and analgesics from wastewater by adsorption on cross-linked β-cyclodextrin

Anna Skwierawska [a,*], Dominika Nowacka [a], Katarzyna Kozłowska-Tylingo [b]

[a] Department of Chemistry and Technology of Functional Materials, Gdańsk University of Technology, Narutowicza 11/12, 80-233, Gdansk, Poland
[b] Department of Pharmaceutical Technology and Biochemistry, Gdańsk University of Technology, Narutowicza 11/12, 80-233, Gdańsk, Poland

ARTICLE INFO

Keywords:
Pharmaceuticals
Shape-memory polymers
Adsorption
Sewage

ABSTRACT

We present a method using the material in the form of cross-linked β-cyclodextrin (CD) showing high efficiency in the simultaneous removal of hazardous pollutants from sewage, such as diclofenac (DIC), ibuprofen (IBU), ketoprofen (KETO), naproxen (NAPR), salicylic acid (SALI) and tramadol (TRAM). The material is stable and particularly easy to regenerate. The sorbent probably remembers the shape of the contaminants, which increases its sorption capacity after the second use. The kinetics of the KETO adsorption process from one-, two- and three-component solutions are well described by the pseudo-second-order model. The maximum polymer capacity was 162.60 mg g^{-1}. The interactions of KETO with CD were investigated, indicating that the main sorption mechanism is based on supramolecular interaction and uptake by a polymer network. The material is not sensitive to low pH and high salinity, so it can be used for the treatment of DIC, IBU, and KETO post-production wastewaters.

1. Introduction

Pharmaceutical industry wastewaters are high variability of composition due to the wide spectrum of manufactured drugs [1,2]. Moreover, the wastewater streams generated during production are characterized by relatively high concentrations of pharmacologically active substances (API) [3]. Often, they have a very low or high pH. Usually, before entering the activated sludge chambers, their composition is averaged by mixing in a homogenizer and pH correction in a neutralizer [4]. At this stage, many pharmaceuticals precipitate out and become less bioavailable [5]. This phenomenon can be counteracted by subjecting the post-production streams to preliminary treatment. The most commonly used are Advanced Oxidation Processes (AOP) [6–10], membrane [11–14], and adsorption methods [15–17]. In the first case, mineralization is very rarely achieved. Typically, the drug is converted into other derivatives that may be less environmentally friendly than the native substance [18,19]. The use of appropriate membranes seems to be a better resolution. Disregarding the high cost, the contaminants are obtained in a form that is easier to dispose of due to the significantly reduced volume [20,21]. Adsorption produces give a similar effect with much less investment. In the pharmaceutical industry, activated carbon (AC) is most often used, both in the product purification stage and in the removal of impurities from waste streams [22–33]. The most important advantages of AC include a large specific surface area and the ability to bind both organic and inorganic compounds. The disadvantages include separation and regeneration problems, especially when using AC in powder form, and final disposal [34]. Waste AC usually undergoes combustion [35]. This process is difficult to carry out due to the lack of volatile

* Corresponding author. Department of Chemistry and Technology of Functional Materials, Gdańsk University of Technology, Narutowicza 11/12, 80-233, Gdańsk, Poland.
E-mail address: anna.skwierawska@pg.edu.pl (A. Skwierawska).

https://doi.org/10.1016/j.wri.2022.100186
Received 9 March 2022; Received in revised form 15 July 2022; Accepted 20 July 2022
Available online 31 July 2022

components and therefore a supply of steam and oxygen is required, thus creating the conditions for gasification [36]. The described procedure is far from green technology and requires the implementation of new ones. A solution that is currently very popular is organic adsorbents derived from renewable raw materials [37–39]. This group includes both dried and shredded plant waste [40,41] as well as cellulose [42–44], chitosan [45–48], and cyclodextrins (CD) [49–51]. The latter is quite soluble and requires appropriate modification. The selection of appropriate cross-linking agents enables the synthesis of an adsorbent tailored to the size of a single or a group of pollutants [52–54]. The basis of sorption is supramolecular interactions produced by van der Waals forces, hydrogen bonds, and molecular fit of guest (pollutant molecule) to host (CD) [53,55]. CDs are cyclic compounds composed of 6, 7, or 8 glucose units linked by α-1,4-acetal bonds [56,57]. The torus is hydrophobic on the inside and hydrophilic on the outside [58]. The hydrophobic parts of the organic compounds are contained inside the torus or, if the structure of the polymer allows it, also in the resulting network. Usually, the materials are durable, regeneration is simple [59–61], and the spent polymer can potentially be broken down during composting, for example [62,63].

This paper presents the possibility of removing ketoprofen directly from post-production wastewater streams. Subsequent experiments show that the composition of wastewater has a significant impact on the efficiency of drug removal. This research can help manage streams going to the homogenizer in industrial wastewater treatment plants. The presented material may also find application in the treatment of municipal wastewater from non-steroidal anti-inflammatory drugs (NSAID) and painkillers.

2. Materials and methods

2.1. Reagents and techniques

Hexamethylene diisocyanate (1,6-HMDI ≥ 99%), β-cyclodextrin (β-CD ≥ 97%), pyridine (anhydrous ≥99.8), diclofenac (DIC), ibuprofen (IBU), ketoprofen (KETO), naproxen (NAPR), paracetamol (PARA), salicylic acid (SALI), tramadol (TRAM) (drugs meet USP testing specifications) were delivered by Sigma-Aldrich. Acetonitrile (HPLC-grade), methanol (CH_3OH ≥ 99.8%), sodium and calcium chlorides (NaCl ≥99.8%, $CaCl_2$ ≥ 99.8%), as well commercial humic acids contain 50% of humic acids and 50% fulvic acids (HA, 90% dry matter) were purchased from Chempur and Agraplant, respectively. All chemicals were used without their further purification. Water purified by Hydrolab-system was used to prepare the stock solutions (HLP-SPRING, temp. 22 °C, κ= 2.70 μS). The characteristic of effluents from the local municipal sewage treatment plant is presented in the supplementary material (SM, Table S2).

The final form of the adsorbent was obtained after drying material in a moisture analyzer (MA50/1.R, Radwag) and grinding in a ball mill (Pulverisette 7 classic line, Fritsch, GmbH). Fourier transform infrared (FT-IR) spectra were performed on a Thermo Nicolet iS10, using the KBr pellet method. The spectral resolution was 4 cm^{-1} and the scanning range was from 400 to 4000 cm^{-1}. The specific surface area was estimated by the Brunauer-Emmett-Teller (BET) method [64] and pore size distribution (PSD) was measured using the classical Barrett-Joyner-Halenda (BJH) model [65] and the Harkins and Jura t-Plot method [66,67]. The surface charge properties of the adsorbents were investigated by Zeta potential measurements, which were conducted at a different equilibrium pH using a Nano-ZS Zetasizer (Malvern Instruments Inc. UK). Thermogravimetric analysis (TGA) and differential scanning calorimetry (DSC) was performed on β-CD-HDMI using a Mettler-Toledo TGA/DSC thermogravimetric analyzer. Samples were heated from 0 °C to 1000 °C at the rate of 10 °C/min under the air atmosphere (flow rate: 10 ml min^{-1}). The surface morphology β-CD-HMDI was studied using scanning electron microscopy (SEM) on a Quanta FEG 250 scanning electron microscope operating at 10 kV. The elemental FLASH 2000 analyzer operating in the dynamic separation technique was used to measure the content of carbon, hydrogen, and nitrogen. The oxygen content analysis was performed by the device in the pyrolysis mode.

2.2. Synthesis of β-CD-HDMI

To a flask containing 150 ml of dry pyridine at 80 °C, 10 g of CD and 5.93 g of 1,6-HMDI were added simultaneously over 2 h with vigorous stirring. Reactions were continued for an additional 8 h. After cooling to room temperature, 300 ml of acetone was poured into the reaction mixture to precipitate the product. The precipitate was filtered and air-dried. Unreacted cyclodextrin and residual pyridine were removed during liquid/solid extraction with water and hydrochloric acid, respectively. The precipitate was filtered and washed with distilled water until the pH of the filtrate was neutral, and then the precipitate was allowed to dry at room temperature. The product was placed in a moisture analyzer and dried at 120 °C until solid. The product thus dried was ground and stored in a desiccator. The final reaction yield was 11.15 g [68].

2.3. Methods

To determine the adsorption mechanism, the interactions between β-CD and API were analyzed through proton nuclear magnetic resonance. ^1H NMR spectra were recorded in D_2O on a Bruker Advance III HD 400 MHz spectrometer at 25 °C.

The concentrations of API were determined by ultraviolet spectra, detected by high-pressure liquid chromatography (HPLC Agilent Technologies 1200 Series, USA). The analytical method for DIC, IBU, KETO, and NAPR was obtained from the reported literature [69–74]. The samples were injected at a volume of 1 μL each time. The flow rate of a mobile phase (using acetonitrile: acetate buffer pH 3.2, ratio 60: 40) through the C-18 column (Zorbax Eclipse PAH, 4.6 x 100 mm, 3.5 μm, Agilent Technologies) was set at 1.0 ml min^{-1}. The concentration was measured by the UV detector at the wavelength of 220.8 (ref. 360 ± 100) nm. TRAM, SALI and PARA were separated on the column XDB C18 Eclipse (4.6 x 150 mm, 5 μm, Agilent Technologies, using mixture of deionize water (A): 0.05% TFA in acetonitrile (B) as a mobile phase, with flow rate 1.2 ml min^{-1} in gradient: 0 min - 85% (A) to 11 min - 40% (A), and back to the

initial conditions (12–17 min - 0% (A)). The samples were injected at a volume of 40 μL. The concentration of analytes was measured by the UV detector at the wavelength of 200.8 (ref. 360 ± 100) nm. All experiments were carried out in triplicate (n = 3) and, the maximum standard error was 2.1%. API removal efficiency (RME) was determined by Eq. (1),

$$RME\ (\%) = \frac{C_0 - C_t}{C_0}\ x\ 100 \tag{1}$$

where the RME (%) was the efficiency of API removal, C_0 (mg L^{-1}) and C_t (mg L^{-1}) were the initial concentration and concentration at time t of API in the sample.

2.4. Adsorption procedure

The experiments were performed at room temperature on a digital vortex mixer (OHAUS VXHDDG) at 700 rpm. After shaking, the adsorbent was separated from the solution by filtration (Whatman Grade 540 filter paper) and the concentration of the filtrate (c_e) was determined. The influence of the adsorbent quantity was initially investigated. For this purpose, β-CD-HMDI in an amount of 1–100 mg was added to 5 ml of KETO solution in plastic Falcon tubes (7 ml). Then, the influence of electrolytes and humic acids, as well as pH 2 to 10 (corrected with NaOH or HCl), was investigated using a previously selected dose of the adsorbent. Each time, three sets of experiments were carried out at the KETO (20 mg L^{-1}, the contact time of 60 min).

2.5. Kinetic, equilibrium studies, and thermodynamic analysis

Kinetic and equilibrium experiments were performed under optimal experimental conditions. In the first one, the KETO (20 mg L^{-1}) solution was used, and in the second - KETO (1–100 mg L^{-1}). The adsorption equilibrium and kinetics data were analyzed using the models presented in Tables S4 and S6. The tables also show the relevant mathematical relations of these models, the parameters to be valued, and the dependable references. The reliability of the results was considered based on the analysis of variance (Anova test).

2.6. Real wastewater treatment

2.6.1. API's post-production effluents

Many methods for synthesizing ketoprofen can be found in the literature [75–80]. However, not all of them are suitable for industrial purposes, which explains the continued use of the syntheses described in patents from the past century [75,81,82]. Fig. 1 shows two examples of the reactions carried out under industrial conditions.

Their common feature is usually an alkaline hydrolysis step carried out in an organic solvent environment, which is then distilled. The resulting drug is in the form of a salt from which it is released. The resulting solution of the drug in the solvent is washed repeatedly with water and solutions of different pH. The combination of these streams produces saline and usually acidic wastewater. A similar situation is observed during the production of diclofenac [83]. The exception is the ibuprofen system, which is considered to be waste-free [84]. The information in the literature has become a determinant of the composition of model post-production leachates (EP) which were prepared by dissolving DIC, IBU, and KETO (0.4 mmol L^{-1}) in a hydrochloric acid solution of sodium chloride (pH=2; 763 mg L^{-1}).

2.6.2. Wastewaters

Model wastewater was obtained by dissolving individual APIs (0.4 mmol L^{-1}) in treated municipal wastewater (MW), the description of MW is shown in Table S1. The resulting mixtures can successfully mimic the feedstock for the next treatment step based on adsorption.

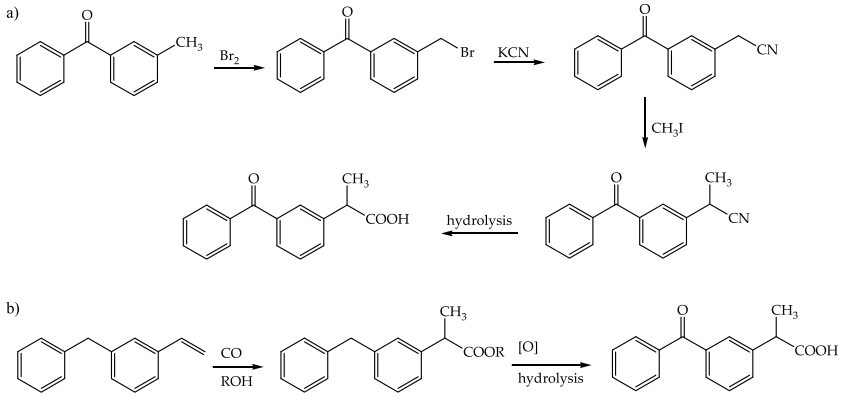

Fig. 1. Industrial methods of ketoprofen synthesis.

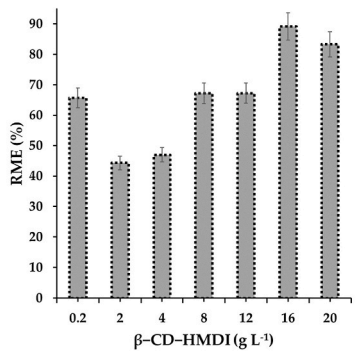

a)

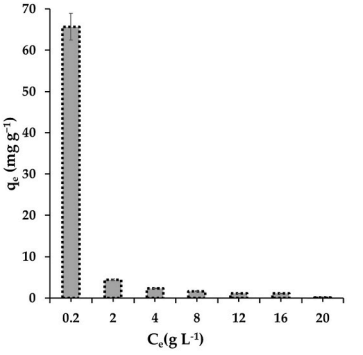

b)

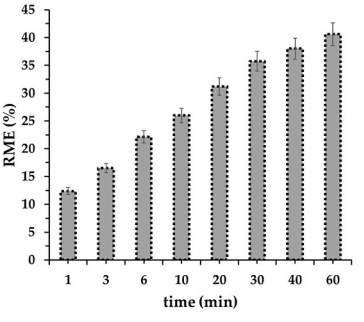

c)

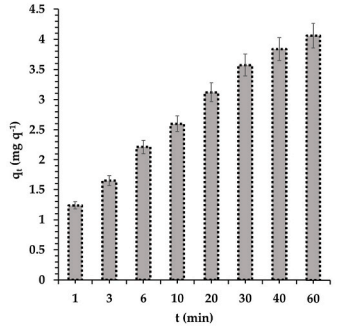

d)

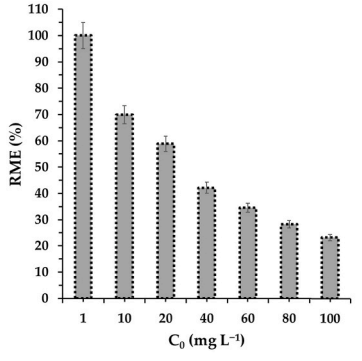

e)

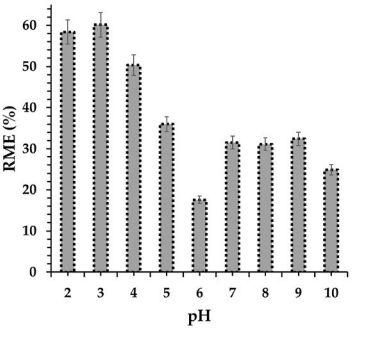

f)

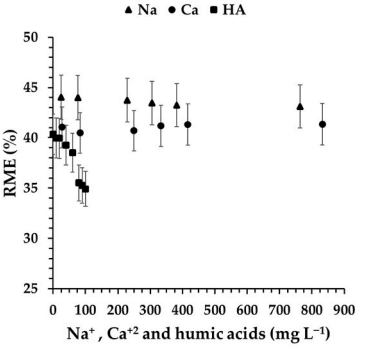

g)

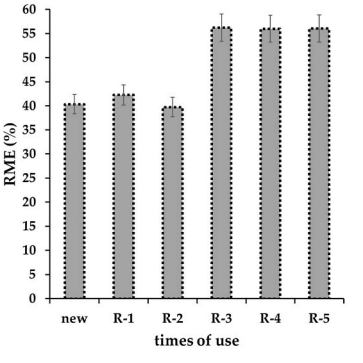

h)

(caption on next page)

Fig. 2. a) Effect of adsorbent mass on removal efficiency, ($C_{\beta\text{-CD-HMDI}}$ =0.2–20 g L^{-1}; C_0 = 20 mg L^{-1}, t = 60 min, temp. 25 °C); b) Effect of adsorbent mass on adsorption capacity, ($C_{\beta\text{-CD-HMDI}}$ = 0.2–20 g L^{-1}; C_0 = 20 mg L^{-1}, t = 60 min, temp. 25 °C); c) Effect of the time on removal efficiency, ($C_{\beta\text{-CD-HMDI}}$ = 0.2–20 g L^{-1}; C_0 = 20 mg L^{-1}, t = 60 min, temp. 25 °C) d) Effect of time on adsorption capacity (q_t), ($C_{\beta\text{-CD-HMDI}}$ = 2 g L^{-1}; C_0 = 20 mg L^{-1}, t = 0–60 min, temp. 25 °C); e) Effect of KETO initial concentration on removal efficiency, ($C_{\beta\text{-CD-HMDI}}$ = 0.2 g L^{-1}; C_0 = 10–100 mg L^{-1}, t = 60 min, temp. 25 °C); f) Effect of pH = 2–10 value on KETO removal efficiency, ($C_{\beta\text{-CD-HMDI}}$ = 2 g L^{-1}; C_0= 20 mg L^{-1}, t = 60 min, temp. 25 °C); g) API Effect of salt and fulvic and humic acids (F&H) on API removal efficiency, ($C_{\beta\text{-CD-HMDI}}$ = 2 g L^{-1}; C_0 = 20 mg L^{-1}, t = 60 min, temp. 25 °C, C_{NaCl} = 25.42–703.00 mg L^{-1}, C_{CaCl2} = 27.75–832.50 mg L^{-1}, $C_{F\&H}$ = 10–100 mg L^{-1}; h) Comparison of the removal efficiency of KETO using a new and sequentially regenerated adsorbent, ($C_{\beta\text{-CD-HMDI}}$ = 2 g L^{-1}; C_0 = 20 mg L^{-1}, t = 60 min, temp. 25 °C). The symbols C_e and q_e denote equilibrium concentrations of KETO in solution and adsorbent, while C_0 and $C_{\beta\text{-CD-HMDI}}$ represent initial concentrations of KETO and adsorbent.

2.6.3. Multicomponent wastewaters (mix)

Ternary blends were prepared by mixing equal volumes of the respective DIC, IBU, and KETO solutions in MW. Seven-component effluents were obtained analogously by mixing all the solutions of the drugs under study.

The aforementioned model effluents (50 ml) were poured into Falcon-type plastic tubes containing 50 mg each of β-CD-HMDI. The vials were sealed tightly, and the mixtures were shaken in a digital vortex mixer at 700 rpm for 1 h at 25 °C. The supernatant was then collected and filtered. The concentration at adsorption equilibrium of each was measured by HPLC.

2.7. Regeneration

100 mg of β-CD-HMDI was added to 50 ml of KETO solution initial (20 mg L^{-1}). The mixture was shaken in a digital vortex mixer at 700 rpm (25 °C, 1 h). After 1 h, the solution was decanted from the surface of the precipitate and in its place, 20 ml of methanol was added, soaking for 15 min. The procedure was repeated in distilled water. The adsorption-desorption experiment was performed five times.

3. Result and discussion

The synthesized material is characterized by a high degree of cross-linking. The basic sorbent unit consists of three β-CD molecules. In a single β-CD, a total of 21 primary hydroxyl groups are available, 16 of which are substituted. Significantly, only 14 are embedded in urethane bonds and two in allophanate bonds. The resulting material is amphiphilic having both rigid and flexible elements (Fig. S13) so it can easily adapt to the structure of the adsorbed drug. The BET surface area of β-CD-HMDI is 7.31 m^2 g^{-1}. The average pore size is 16.8 nm and the total pore volume is 3.08 ml g^{-1}. The average particle size of β-CD-HMDI varieties is from 270 to 600 μm, valued by SEM (Fig. S2). The particles have a divergent porous structure. The material is thermally stable at temperatures below 250 °C, after which decomposition follows. The final weight loss is observed at 333 °C (61.82%). The Zeta potential (ξ) of β-CD-HMDI in the pH range from 2 to 11 is 0 for pH = 2.53, and above this value, it is constantly negative. The material does not permanently retain water and does not tend to swell. More information on the sugar adsorbent can be found in the publication [68].

3.1. Adsorption experiments

The adsorption studies were carried out conventionally, examining the influence of individual parameters on the course of the process. The obtained results are discussed in subsequent subsections.

3.1.1. Effect of adsorbent mass

It can be considered that overall, an increase in the mass of the sorbent (0.2–20 g L^{-1}) is accompanied by an increase in the degree of removal of API from the solution, which is certainly typical. Nevertheless, in the case of KETO, it reaches minimums and maximums, which indicate probably the formation of new equilibria (Fig. 2a). A significant excess of API in the solution compared to the initial amount of β-CD-HMDI causes a rapid equilibrium state where the q_e limits of 65.42 mg g^{-1} (Fig. 2b). Therefore, to be able to investigate the kinetics of the sorption process, no minimum amount of material, but 10 mg was used in the next stage. The pH of the API solutions (20 mg L^{-1}) was not corrected.

3.1.2. Effect of contact time

The adsorption processes are required to run efficiently in a relatively short time to reduce the cost of the unit operation. The time in which the maximum removal of the desired component from solution was achieved depends on the kinetics of the process, which is predominantly influenced by the physicochemical properties of the adsorbent and adsorbate. In the KETO question, the required state was achieved in between 5 min and 24 h, depending on the material used [85–87]. Two compartments can be distinguished in the analyzed system. The first one, lasting 30 min, is dynamic, then it slows down significantly. The result is a 40.62% removal of KETO in 60 min (Fig. 2c).

3.1.3. Effect of API initial concentration

The initial concentration is the driving force needed to overcome the resistance to mass transfer between the aqueous and solid phases. At the first moment of contact, β-CD-HMDI has the largest number of centers capable of interacting with the components of the liquid phase, which usually results in a high adsorption efficiency observed at the lowest concentration of 1 mg L^{-1}. A higher

concentration may create an additional barrier to overcome in the form of already accumulated KETO particles, or API transfer from solution to solid. Hence, the involvement of deeper structures is partial, and consequently, the ineffectiveness of API removal is observed. The concentration of 20 mg L^{-1} was selected for further research (Fig. 2e).

3.1.4. Effect of pH

KETO contains a pH-sensitive carboxyl group. In a solution with pH = 3, the degree of API removal is the highest and amounts to almost 61% (Fig. 2f), then it gradually decreases with increasing pH, assuming the lowest value for pH = 6 (RME = 17.55%), after which, when exceeded, there is an almost two-fold increase to pH = 9. The electrokinetic potential of the various dispersed phases depends largely on the concentration of hydrogen ions. In the case of the tested material, the electrokinetic potential is zero at pH = 2.53, this value corresponds to the highest degree of KETO removal (Fig. S3). This is an area close to the complete disappearance of anticoagulant electrostatic repulsion. Considering that the final pH of the effluent from KETO production is acidic and the drug content is at the level of several dozen mg, the resulting material can potentially be used to remove the drug from this stream before it is sent to the on-site sewage treatment plant [81]. However, to restore normal adsorption conditions, the pH of the KETO solutions was not adjusted in further tests and was 4.21.

3.1.5. Effect of salts, humic and fulvic acids

The salts present in the wastewater can significantly affect the sorption of drugs. In the case of KETO, both sodium and calcium chloride increase the removal efficiency of the drug by several percent. Even high salinity mustn't adversely affect the sorption process, which means that β-CD-HMDI can potentially be used during the treatment of neutralized post-production wastewater. The presence of humic and fulvic acids is typical for surface waters and may be of great importance when removing KETO from the natural environment. These compounds have little effect on the value of the RME parameter in the range of low concentrations, the effect increases with increasing concentration, resulting in a reduction in the degree of KETO removal by 5% (Fig. 2g).

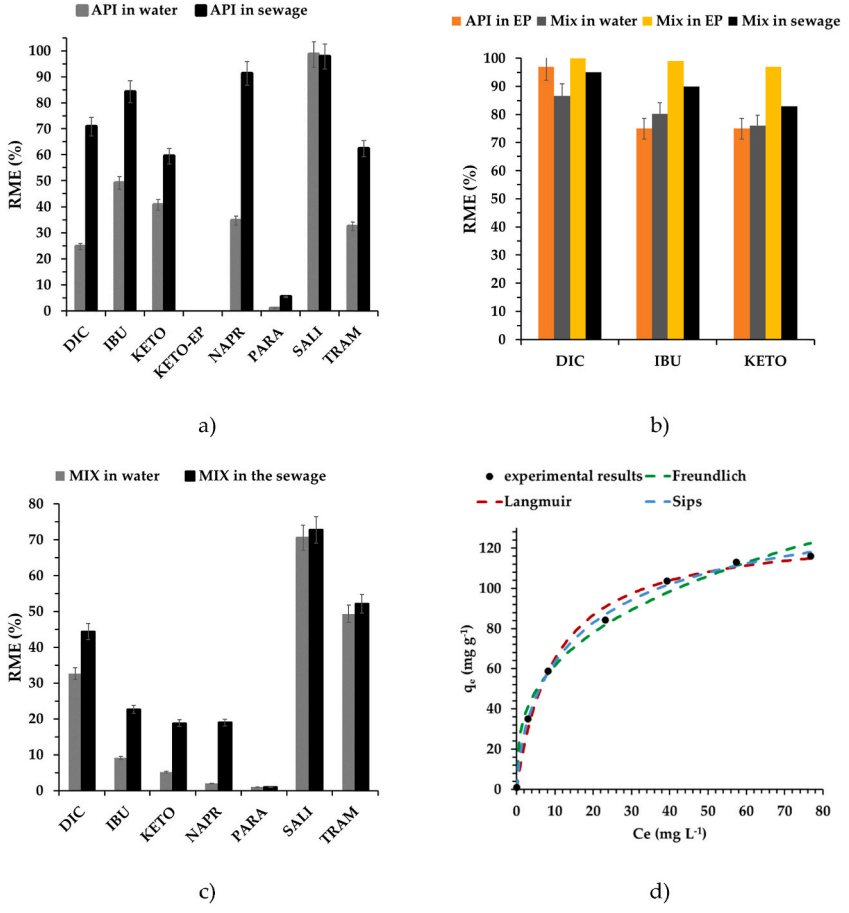

Fig. 3. a) The removal efficiency of single API from water and municipal wastewater; b) Removal of drugs from three-component mixtures in water, post-production effluent (EP), and municipal wastewater; c) Removal of drugs from seven-component mixtures in water and municipal sewage. In all cases $C_{API} = 0.3\ mmol\ L^{-1}$, $C_{\beta-CD-HMDI} = 1.25\ g\ L^{-1}$ contact time 60 min, temp. 25 °C; d) Equilibrium adsorption isotherm of KETO ($C_0 = 0.001-0.1\ g\ L^{-1}$, $C_{\beta-CD-HMDI} = 0.2\ g\ L^{-1}$, contact time 60 min, temp. 25 °C).

3.1.6. Regeneration

The presented material contains elements of different elasticity, enabling a better adjustment of the material structure to the shape of the adsorbate. The initial structure of β-CD-HMDI was formed by a pyridine matrix which was removed in the purification step. During the first sorption, the material is reorganized and arranged according to the structure of the guest molecule. The new system is not fully formed but does not fail under mild methanol desorption conditions. During the next two cycles (adsorption-desorption), the new polymer system is remembered and the process becomes more efficient (Fig. 2h). The low boiling point of alcohol and the lack of azeotropes with water make the regeneration stage relatively cheap and waste-free. The regeneration process must be very effective and simple. In industrial conditions, it is enough to place the sorbent in the mixer with post-production effluents. After an appropriate time, it is enough to drain the treated sewage and replace it with methanol, after only 15 min, the solvent phase can also be drained and sent to the distillation tower, and the material itself can be washed with water. The operation does not need to be repeated. Aqueous washings can also be used repeatedly after removing residual methanol (Scheme S1).

3.1.7. Removal of pollutants from a complex model mixture

The presence of additional drugs such as DIC and IBU increases the removal efficiency of the individually tested API from model solutions. This effect is strongest with DIC, which is removed from the solution with an efficiency of 24.7% in the absence of other drugs. In the case of a mixture containing all tested pharmaceuticals, the effectiveness increases up to 86.6%. The observed synergism of these drug adsorption is an unquestionable advantage of β-CD-HMDI and has the potential to be used in the treatment of combined post-production wastewater from the simultaneous manufacture of these medicines (Fig. 3a and b and Scheme S1).

3.1.8. Adsorption of pharmaceuticals present in biologically treated sewage of municipal type and post-productions streams

The composition of the wastewater depends on the source of its formation. Two cases of mixtures containing API were included in the research. The first one with the pH = 2 and sodium chloride (763 mg L^{-1}) is the simulation of the KETO adsorption process from post-production effluents [81]. The second is the removal of drugs from municipal wastewater. First, the effect of the matrices on the removal efficiency of single APIs was determined, followed by mixtures containing three or seven drugs (concentration 0.3 mmol L^{-1} each). Components of municipal wastewater have a positive effect on the removal of API from wastewater containing single pharmaceuticals (Fig. 3a). The degree of KETO removal is similar to that in the presence of salt and humic acids. The phenomenon of low PARA adsorption is difficult to explain, especially as it complexes with β-CD (Fig. S10), like other studies (Figs. S6, S7, S8, S9, S11, S12) [88,89]. Perhaps interactions under environmental conditions are unstable or the matrix contains more attractive substances.

The three-component mixtures (DIC, IBU, and KETO) are noteworthy as they indicate the synergism of the mentioned compounds also under environmental conditions, which effectively eliminates the influence of the matrices. The result is a high removal rate for each drug, slightly higher than that of distilled water solutions (Fig. 3b). The efficiency of removing these APIs from synthetic production wastewater is impressively high for single production streams as well as their mixtures (Fig. 3b). Cyclodextrin materials do not have functional groups sensitive to low pH, and the hydrophobic interior is not attractive to salt, hence the lack of sensitivity to the high salinity of the formed supramolecular complexes. This could be expected based on the previously conducted studies on the effect of pH and sodium chloride on the sorption efficiency of the drug (Fig. 2f and g). β-CD-HMDI is a material whose action is based primarily on the formation of supramolecular complexes, characterized by various durability. It is no wonder that for more complex systems we can see completely different results, such as for mixtures formed by dissolving DIC, IBU, KETO, NAPR, PARA, SALI, and TRAM in water or wastewater, respectively. The APIs used for comparison also belong to the group of hazardous pollutants commonly found in the natural environment, which justifies the choice [90–93]. The presence of seven pharmaceuticals in the mixture significantly reduced the influence of the matrix on adsorption compared to the one-component systems. The strongest interactions with the β-CD-HMDI surface are observed in the case of SALI and TRAM, which are removed with an efficiency of 72.7% and 52.1%, respectively. Unfortunately, the degree of removal of the remaining ones decreased in a relatively high concentration range (Fig. 3c).

3.1.9. Adsorption isotherms

The isotherm shown in Fig. 3d corresponds to type I. The course of the isotherm reflects the basic assumptions of Langmuir's theory that the adsorbent surface has many active sites, and only one adsorbate molecule can adsorb to one active site. The amount of adsorption initially increases in proportion to the concentration of the adsorbate, then the increase gradually decreases and the adsorption becomes constant. All active places are occupied and a monolayer is formed. A larger amount of the adsorbate particles cannot be adsorbed on the adsorbent surface. Using the nonlinear and linear form of the Langmuir equation, the maximum adsorption capacity (q_{max}) was determined, amounting to 129.70 mg L^{-1} and 131.23 mg L^{-1}, respectively. This value is higher than that resulting from the β-CD content in the polymer structure (54%) [68], which indicates the existence of non-supramolecular interactions. An important addition to the Langmuir isotherm is the dimensionless separation factor R_L. The calculated value shows the privileged course of the process $0 < R_L < 1$ (Table S4). The Freundlich model was also used to eliminate or confirm multilayer adsorption involving inhomogeneous surfaces with non-uniform heat distribution of adsorption. The parameter n, which is decisive for the quality of the adsorption process, was estimated based on its linear form. When its value is in the range of 1–10, the process is preferable in that case. However, the determined statistical coefficients indicate a worse fit of the experimental points to the model (Table S5). The Sips model is a sense of balance to those described and works well for localized adsorption without adsorbate-adsorbate interaction [94,95]. As C_e approaches a low value, the Sips isotherm transforms into Freundlich, and at high C_e into Langmuir. The Sips isotherm equation is also characterized by the dimensionless heterogeneity coefficient n, which can be used to describe the heterogeneity of the system if the value of n is from 0 to 1. In the case under consideration, $n = 0.71$(nonlinear) and $n = 1.43$ (linear). The linear model may show a relationship between adsorbent and adsorbed molecules. The β-CD-HMDI - KETO system is perfectly suited to the Sips model as

evidenced by the error analysis and the value of the linear regression coefficient (Table S5). Based on the nonlinear and linear form of the Sips isotherm, the value of $q_{max} = 161.13$ mg L^{-1} and $q_{max} = 162.60$ mg L^{-1} was determined, which is higher than that resulting from the Langmuir equation. This obtained q_{max} value was compared with the maximum sorption capacity of other sorbent materials for KETO reported in the literature and presented in Table 1. Of these, only nitrogen-doped reduced graphene has a higher q_{max} than β-CD-HMDI. It should be noted that in the case of β-CD-HMDI the adsorption process is more efficient considering the short adsorption time and five times the lower specific surface area. In addition, β-CD-HMDI maintains a constant sorption capacity in subsequent cycles and the regeneration itself is fast and simple.

3.1.10. Thermodynamic analysis

The obtained negative value of ΔH° means that the process is exothermic and proceeds with energy release. Negative ΔG° values point to unprompted and thermodynamically favorable processes as well as an affinity of the adsorbate for the adsorbent [101]. Positive values of ΔS° specify a high preference for the adsorbate molecules on the adsorbent surface [102] (Table S5).

3.2. Kinetic models

Seven classical models of adsorption kinetics were used to fit the data: pseudo-first order, pseudo-second order, Elovic, modified Freundlich, Weber Morris (intramolecular diffusion), Bangham pore diffusion, and liquid layer diffusion (Table S5). Considering the fit to the model based on the statistical analysis, it can be concluded that the pseudo-first-order model best describes the adsorption of KETO, $R^2 > 0.998$. (Table S7). Nevertheless, the value of q_e estimated based on this model deviates significantly from the experimental value (Fig. 2d), which is close to q_e calculated from the pseudo-second-order model (Table S6). Three more models were used to determine the limiting stage of the process. The results obtained after fitting the experimental data to these models indicate that the diffusion of the boundary layer (film) and inside the surface of solid particles (pores), substances dissolved in the solution, are equally important. A long time to reach the adsorption equilibrium (approx. 1 h) may indicate that internal diffusion dominates the overall adsorption kinetics. To confirm unequivocal information about the reaction rate limitation, the assumptions of Weber and Morris based on an internal diffusion model [103,104] were used. This model describes the equation shown in Table S6, *the* k_{id} is the intra-particle diffusion rate constant and C is the layer thickness. The higher the value of C, the greater the influence of the boundary layer on the adsorption process. If the rate-limiting factor is diffusion inside the particles, then the dependence of the square root function q_t on the time $t^{1/2}$ is a straight line passing through the origin of the coordinate system, i.e. C = 0. In the case under consideration, C = 1.05, which markers that the rate-limiting factor is the boundary layer (film) controlled by the diffusion process (Table S7). Additional applied Elovic and modified Freundlich models during fitting experimental data were linear over the entire range, and the slopes describing the modified Freundlich kinetic model significantly below the value of unity confirm the chemisorption of KETO at a concentration of 20 mg L^{-1} (Table S7).

The presence of additional APIs results in a better fit to the pseudo-second-order kinetic model of each of the drugs under consideration (Table S8). Two-component mixtures are characterized by a significantly higher rate of removal of organic compounds and better use of the specific surface area of the material (Fig. S5). In the case of three-component mixtures, the highest degree of drug removal is observed as well as adsorption rates (Fig. S5 and Table S8). DIC pseudo-second-order reaction constant k_{2-DIC} increases almost 581-fold, k_{2-IBU} 7.7-fold, and k_{2-KETO} 72-fold, respectively. Conceivably this phenomenon is accompanied by changes in the structure of the material, which make it possible to significantly accelerate the adsorption of the most spatial molecules, i.e. DIC.

3.3. Mechanism of adsorption

To put it simply, all tested pharmaceuticals form supramolecular complexes with β-CD both in the solid phase and in aqueous solutions [88,105–108], so they should also be retained in the β-CD-HMDI structure. Six out of seven do. The exception is paracetamol, which forms a 3: 2 stoichiometry complex with CD in aqueous solutions (Fig. S10). The formation of a multi-component complex requires the appropriate mutual arrangement of the molecules that make up the compound. Cross-linking significantly reduces the number of degrees of freedom of the β-CD rings and requires a different arrangement. Consequently, the interactions are so weak that PARA is equally quickly adsorbed and desorbed. In the sorption process, the stoichiometry of the resulting complex is not the only

Table 1
Examples of adsorbents used to remove KETO from waters.

Adsorbent type	Q_{max} (mg g^{-1})	pH	Temp. (°C)	Time (h)	Specific surface area (m^2 g^{-1})	Reference
Sonicated activated carbon	40.0	2.0	25	2	640.9	[27]
Montmorillonite	67.0	6.4	25	2	32.0	[96]
Carbon nanotubes	99.0	4.5	25	24	170.9	[97]
Activated carbon prepared from effluent treatment plant sludge of the beverage industry	105.9	4.0	25	3	642	[98]
activated carbon prepared from winery wastes	146.4	3	25	6	227.16	[99]
β-CD-HMDI	**(161.13) 162.60**	**4.2**	**25**	**1**	**7.3**	**This work**
Nitrogen-doped reduced graphene oxide modified by Fe_3O_4	468.0	6.8	25	24	38.20	[100]

significant component. SALI in aqueous solutions also forms 3: 2 complexes with β-CD (Fig. S11) and, interestingly, shows the highest affinity for the material in both aqueous solutions and sewage. The explanation should be sought in the arrangement of the functional groups. Most likely, the aromatic rings of the acid are located in the β-CD tori, while its functional groups, located in the ortho position to each other, are involved in the formation of a network of hydrogen bonds with other elements of the sorbent structure. The remaining APIs show greater lipophilicity due to the presence of aliphatic or aromatic substituents, thereby increasing the number of possible structures (Fig. S6-S12 and S13). For example, the phenolic substituent KETO is complexed through the interior of the CD, the second ring interacts with the aliphatic chain of the lattice, and the carboxyl group is involved in hydrogen bonding with the urethane or allophanate moiety (Fig. S13).

4. Conclusions

The paper presents a material that, contrary to the commonly used activated carbons in the form of a powder, is easily separated and regenerated. It is durable and can work in environmental conditions. The sorption capacity remains unchanged after the next five regeneration cycles. Despite the small specific surface area of the material, a high degree of KETO removal from model post-production effluents is achieved during the simultaneous removal of diclofenac, ibuprofen, and ketoprofen, even in concentrations much higher than those found in the natural environment, which allows it to be used in industrial conditions. The outflow of streams from municipal wastewater treatment plants containing the above-mentioned drugs can be successfully purified, achieving efficiencies in removing diclofenac, ibuprofen, and ketoprofen of 95%, 82%, and 78%, respectively. Even higher efficiency of the pre-treatment can be obtained in industrial conditions by combining the streams of the above-mentioned APIs (100% DIC, 99% IBU, and 97% KETO). The presence of additional other NSAIDs and analgesics in the wastewater modifies the adsorption profile, and the preferred adsorbent compounds are mainly salicylic acid, tramadol, and diclofenac, for which the removal efficiencies are 72%, 52%, and 44%, respectively.

CRediT authorship contribution statement

Anna Skwierawska: Conceptualization, Methodology, Investigation, Formal analysis, Validation, Writing - original draft, Visualization, Writing - review & editing.

Dominika Nowacka: Investigation, Writing - review & editing.

Katarzyna Kozłowska-Tylingo: Formal analysis, Validation.

Declaration of competing interest

The authors declare that they have no known competing financial interests or personal relationships that could have appeared to influence the work reported in this paper.

Acknowledgments

The authors are grateful for the financial support provided by Gdansk University of Technology, SB 034016. The authors would like to thank MSc Dominika Nowacka, MSc Paulina Nowicka, and MSc Sandra Rosa for their help in the experimental work.

Appendix A. Supplementary data

Supplementary data to this article can be found online at https://doi.org/10.1016/j.wri.2022.100186.

References

[1] M. Patel, R. Kumar, K. Kishor, T. Mlsna, C.U. Pittman, D. Mohan, Pharmaceuticals of emerging concern in aquatic systems: chemistry, occurrence, effects, and removal methods, Chem. Rev. 119 (2019) 3510–3673, https://doi.org/10.1021/acs.chemrev.8b00299.

[2] C. Gadipelly, A. Pérez-González, G.D. Yadav, I. Ortiz, R. Ibáñez, V.K. Rathod, K.V. Marathe, Pharmaceutical industry wastewater: review of the technologies for water treatment and reuse, Ind. Eng. Chem. Res. 53 (2014) 11571–11592, https://doi.org/10.1021/ie501210j.

[3] V. Kumari, A.K. Tripathi, Characterization of pharmaceuticals industrial effluent using GC–MS and FT-IR analyses and defining its toxicity, Appl. Water Sci. 9 (2019) 1–8, https://doi.org/10.1007/s13201-019-1064-z.

[4] H. Feng, Research progress in pharmaceutical wastewater treatment technology, E3S Web Conf. 118 (2019), https://doi.org/10.1051/e3sconf/201911804019.

[5] J.C. Dearden, R.M. Nicholson, Qsar study of the fate of pharmaceutical chemicals in an aquatic environment, J. Pharm. Pharmacol. 37 (1985), https://doi.org/10.1111/j.2042-7158.1985.tb14143.x, 71P-71P.

[6] C. Ferhan, A. Ozgur, Related Titles Ozonation of Water and Waste Water Introduction to Environmental Engineering Rapid Chemical and Biological Techniques for Water Monitoring Functional Nanostructured Materials and Membranes for Water Treatment Risk Analysis of Water Pollution, 2011.

[7] V. Homem, L. Santos, Degradation and removal methods of antibiotics from aqueous matrices - a review, J. Environ. Manag. 92 (2011) 2304–2347, https://doi.org/10.1016/j.jenvman.2011.05.023.

[8] E.M. Cuerda-Correa, M.F. Alexandre-Franco, C. Fernández-González, Advanced oxidation processes for the removal of antibiotics from water, Overview, Water (Switzerland) (2020) 12, https://doi.org/10.3390/w12010102.

[9] S.S. Boxi, S. Paria, Visible light induced enhanced photocatalytic degradation of organic pollutants in aqueous media using Ag-doped hollow TiO2 nanospheres, RSC Adv. 5 (2015) 37647–37668, https://doi.org/10.1039/c5ra03421c.

[10] L. Jothinathan, J. Hu, Kinetic evaluation of graphene oxide based heterogeneous catalytic ozonation for the removal of ibuprofen, Water Res. 134 (2018) 63–73, https://doi.org/10.1016/j.watres.2018.01.033.
[11] S. Shi, X. Liu, W. Li, Z. Li, G. Tu, B. Deng, C. Liu, Tuning the biodegradability of chitosan membranes: characterization and conceptual design, ACS Sustain. Chem. Eng. 8 (2020) 14484–14492, https://doi.org/10.1021/acssuschemeng.0c04585.
[12] Q. Gui, Q. Ouyang, J. Zhang, S. Shi, X. Chen, Ultrahigh flux and strong affinity poly(N - vinylformamide)-grafted polypropylene membranes for continuous removal of organic micropollutants from water. https://doi.org/10.1021/acsami.1c02507, 2021.
[13] L. Moulahcene, M. Skiba, F. Bounoure, M. Benamor, N. Milon, F. Hallouard, M. Lahiani-Skiba, New polymer inclusion membrane containing β-Cyclodextrin polymer: application for pharmaceutical pollutant removal from wastewater, Int. J. Environ. Res. Publ. Health 16 (2019), https://doi.org/10.3390/ijerph16030414.
[14] L.N. Breitner, K.J. Howe, D. Minakata, Effect of functional chemistry on the rejection of low-molecular weight neutral organics through reverse osmosis membranes for potable reuse, Environ. Sci. Technol. (2019), https://doi.org/10.1021/acs.est.9b03856, 1DUMMY.
[15] R. Lotfi, B. Hayati, S. Rahimi, A.A. Shekarchi, N.M. Mahmoodi, A. Bagheri, Synthesis and characterization of PAMAM/SiO 2 nanohybrid as a new promising adsorbent for pharmaceuticals, Microchem. J. 146 (2019) 1150–1159, https://doi.org/10.1016/j.microc.2019.02.048.
[16] M. Rosset, L.W. Sfreddo, G.E.N. Hidalgo, O.W. Perez-Lopez, L.A. Féris, Adsorbents derived from hydrotalcite for the removal of diclofenac in wastewater, Appl. Clay Sci. 175 (2019) 150–158, https://doi.org/10.1016/j.clay.2019.04.014.
[17] M. Ulfa, N.S. Worabay, M.F. Pradipta, D. Prasetyoko, Removal of ibuprofen from aqueous solutions by adsorption on tiny zinc oxide sheet-like structure, AIP Conf. Proc. (2019) 2194, https://doi.org/10.1063/1.5139863.
[18] R. Zhou, T. Li, Y. Su, T. Ma, L. Zhang, H. Ren, Oxidative removal of metronidazole from aqueous solution by thermally activated persulfate process: kinetics and mechanisms, Environ. Sci. Pollut. Control Ser. 25 (2018) 2466–2475, https://doi.org/10.1007/s11356-017-0518-9.
[19] F. Görmez, Ö. Görmez, B. Gözmen, D. Kalderis, Degradation of chloramphenicol and metronidazole by an electro-Fenton process using graphene oxide-Fe3O4 as heterogeneous catalyst, J. Environ. Chem. Eng. 7 (2019), 102990, https://doi.org/10.1016/j.jece.2019.102990.
[20] Shivani Garg, Advanced industrial wastewater treatment and reclamation of water. https://link.springer.com/10.1007/978-3-030-83811-9, 2022.
[21] Veolia, PHARMACEUTICAL, 2020.
[22] A. Bonilla-Petriciolet, D.I. Mendoza-Castillo, H.E. Reynel-Ávila, Adsorption Processes for Water Treatment and Purification, 2017, https://doi.org/10.1007/978-3-319-58136-1.
[23] B.Y.Z. Hiew, L.Y. Lee, K.C. Lai, S. Gan, S. Thangalazhy-Gopakumar, G.T. Pan, T.C.K. Yang, Adsorptive decontamination of diclofenac by three-dimensional graphene-based adsorbent: response surface methodology, adsorption equilibrium, kinetic and thermodynamic studies, Environ. Res. 168 (2019) 241–253, https://doi.org/10.1016/j.envres.2018.09.030.
[24] D. Bahamon, L. Carro, S. Guri, L.F. Vega, Computational study of ibuprofen removal from water by adsorption in realistic activated carbons, J. Colloid Interface Sci. 498 (2017) 323–334, https://doi.org/10.1016/j.jcis.2017.03.068.
[25] A.O. Abo El Naga, M. El Saied, S.A. Shaban, F.Y. El Kady, Fast removal of diclofenac sodium from aqueous solution using sugar cane bagasse-derived activated carbon, J. Mol. Liq. 285 (2019) 9–19, https://doi.org/10.1016/j.molliq.2019.04.062.
[26] S. Jodeh, F. Abdelwahab, N. Jaradat, I. Warad, W. Jodeh, Adsorption of diclofenac from aqueous solution using Cyclamen persicum tubers based activated carbon (CTAC), J. Assoc. Arab Univ. Basic Appl. Sci. 20 (2016) 32–38, https://doi.org/10.1016/j.jaubas.2014.11.002.
[27] A.C. Fröhlich, E.L. Foletto, G.L. Dotto, Preparation and characterization of NiFe2O4/activated carbon composite as potential magnetic adsorbent for removal of ibuprofen and ketoprofen pharmaceuticals from aqueous solutions, J. Clean. Prod. 229 (2019) 828–837, https://doi.org/10.1016/j.jclepro.2019.05.037.
[28] A.A. Cuthbertson, S.Y. Kimura, H.K. Liberatore, R.S. Summers, D.R.U. Knappe, B.D. Stanford, J.C. Maness, R.E. Mulhern, M. Selbes, S.D. Richardson, Does granular activated carbon with chlorination produce safer drinking water? From disinfection byproducts and total organic halogen to calculated toxicity, Environ. Sci. Technol. 53 (2019) 5987–5999, https://doi.org/10.1021/acs.est.9b00023.
[29] K. Yang, L. Zhu, J. Yang, D. Lin, Adsorption and correlations of selected aromatic compounds on a KOH-activated carbon with large surface area, Sci. Total Environ. 618 (2018) 1677–1684, https://doi.org/10.1016/j.scitotenv.2017.10.018.
[30] T.L. Adewoye, O.O. Ogunleye, A.S. Abdulkareem, T.O. Salawudeen, J.O. Tijani, Optimization of the adsorption of total organic carbon from produced water using functionalized multi-walled carbon nanotubes, Heliyon 7 (2021), e05866, https://doi.org/10.1016/j.heliyon.2020.e05866.
[31] H. Mansouri, R.J. Carmona, A. Gomis-Berenguer, S. Souissi-Najar, A. Ouederni, C.O. Ania, Competitive adsorption of ibuprofen and amoxicillin mixtures from aqueous solution on activated carbons, J. Colloid Interface Sci. 449 (2015) 252–260, https://doi.org/10.1016/j.jcis.2014.12.020.
[32] J. Bedia, M. Peñas-Garzón, A. Gómez-Avilés, J.J. Rodriguez, C. Belver, Review on activated carbons by chemical activation with FeCl3, C — J. Carbon Res. 6 (2020) 21, https://doi.org/10.3390/c6020021.
[33] A.C. Fröhlich, G.S. dos Reis, F.A. Pavan, É.C. Lima, E.L. Foletto, G.L. Dotto, Improvement of activated carbon characteristics by sonication and its application for pharmaceutical contaminant adsorption, Environ. Sci. Pollut. Control Ser. 25 (2018) 24713–24725, https://doi.org/10.1007/s11356-018-2525-x.
[34] D. Balarak, F. Mostafapour, H. Akbari, A. Joghtaei, Adsorption of amoxicillin antibiotic from pharmaceutical wastewater by activated carbon prepared from Azolla filiculoides, J. Pharmaceut. Res. Intern. 18 (2017) 1–13, https://doi.org/10.9734/jpri/2017/35607.
[35] N. Hossain, M.A. Bhuiyan, B.K. Pramanik, S. Nizamuddin, G. Griffin, Waste materials for wastewater treatment and waste adsorbents for biofuel and cement supplement applications: a critical review, J. Clean. Prod. 255 (2020), https://doi.org/10.1016/j.jclepro.2020.120261.
[36] A.D. Kamble, V.K. Saxena, P.D. Chavan, V.A. Mendhe, Co-gasification of coal and biomass an emerging clean energy technology: status and prospects of development in Indian context, Int. J. Min. Sci. Technol. 29 (2019) 171–186, https://doi.org/10.1016/j.ijmst.2018.03.011.
[37] S. Alipoori, H. Rouhi, E. Linn, H. Stumpfl, H. Mokarizadeh, M.R. Esfahani, A. Koh, S.T. Weinman, E.K. Wujcik, Polymer-based devices and remediation strategies for emerging contaminants in water, ACS Appl. Polym. Mater. 3 (2021) 549–577, https://doi.org/10.1021/acsapm.0c01171.
[38] T. Trends, F. Younas, A. Mustafa, Z. Ur, R. Farooqi, X. Wang, S. Younas, W. Mohy-ud-din, M.A. Hameed, M.M. Abrar, A.A. Maitlo, S. Noreen, M.M. Hussain, Environ. Implicat. (2021) 1–25.
[39] H.B. Quesada, A.T.A. Baptista, L.F. Cusioli, D. Seibert, C. de Oliveira Bezerra, R. Bergamasco, Surface water pollution by pharmaceuticals and an alternative of removal by low-cost adsorbents: a review, Chemosphere 222 (2019) 766–780, https://doi.org/10.1016/j.chemosphere.2019.02.009.
[40] R. Lafi, A. ben Fradj, A. Hafiane, B.H. Hameed, Coffee waste as potential adsorbent for the removal of basic dyes from aqueous solution, Kor. J. Chem. Eng. 31 (2014) 2198–2206, https://doi.org/10.1007/s11814-014-0171-7.
[41] O.S. Bello, O.C. Alao, T.C. Alagbada, O.S. Agboola, O.T. Omotoba, O.R. Abikoye, A renewable, sustainable and low-cost adsorbent for ibuprofen removal, Water Sci. Technol. 83 (2021) 111–122, https://doi.org/10.2166/wst.2020.551.
[42] M.A. Ahsan, M.T. Islam, M.A. Imam, A.H.M.G. Hyder, V. Jabbari, N. Dominguez, J.C. Noveron, Biosorption of bisphenol A and sulfamethoxazole from water using sulfonated coffee waste: isotherm, kinetic and thermodynamic studies, J. Environ. Chem. Eng. 6 (2018) 6602–6611, https://doi.org/10.1016/j.jece.2018.10.004.
[43] A.M. Ares, R. Muiño, A. Costoya, R.A. Lorenzo, A. Concheiro, A.M. Carro, C. Alvarez-Lorenzo, Cyclodextrin-functionalized cellulose filter paper for selective capture of diclofenac, Carbohydr. Polym. 220 (2019) 43–52, https://doi.org/10.1016/j.carbpol.2019.05.055.
[44] E. Abu-Danso, A. Bagheri, A. Bhatnagar, Facile functionalization of cellulose from discarded cigarette butts for the removal of diclofenac from water, Carbohydr. Polym. 219 (2019) 46–55, https://doi.org/10.1016/j.carbpol.2019.04.090.
[45] Y. Lu, Z. Wang, X. Kun Ouyang, C. Ji, Y. Liu, F. Huang, L.Y. Yang, Fabrication of cross-linked chitosan beads grafted by polyethylenimine for efficient adsorption of diclofenac sodium from water, Int. J. Biol. Macromol. 145 (2020) 1180–1188, https://doi.org/10.1016/j.ijbiomac.2019.10.044.
[46] Y. Lu, L. Fan, L.Y. Yang, F. Huang, X. Kun Ouyang, PEI-modified core-shell/bead-like amino silica enhanced poly (vinyl alcohol)/chitosan for diclofenac sodium efficient adsorption, Carbohydr. Polym. 229 (2020), 115459, https://doi.org/10.1016/j.carbpol.2019.115459.
[47] W. Phasuphan, N. Praphairaksit, A. Imyim, Removal of ibuprofen, diclofenac, and naproxen from water using chitosan-modified waste tire crumb rubber, J. Mol. Liq. 294 (2019), 111554, https://doi.org/10.1016/j.molliq.2019.111554.

[48] J.M.N. dos Santos, C.R. Pereira, E.L. Foletto, G.L. Dotto, Alternative synthesis for ZnFe 2 O 4/chitosan magnetic particles to remove diclofenac from water by adsorption, Int. J. Biol. Macromol. 131 (2019) 301–308, https://doi.org/10.1016/j.ijbiomac.2019.03.079.
[49] A.M. Khalil, T. Hashem, A. Gopalakrishnan, A.I. Schäfer, Cyclodextrin composite nanofiber membrane: impact of the crosslinker type on steroid hormone micropollutant removal from water, ACS Appl. Polym. Mater. (2021), https://doi.org/10.1021/acsapm.1c00231.
[50] T.F. Cova, D. Murtinho, R. Aguado, A.A.C.C. Pais, A.J.M. Valente, Cyclodextrin polymers and cyclodextrin-containing polysaccharides for water remediation, Polysaccharides 2 (2021) 16–38, https://doi.org/10.3390/polysaccharides2010002.
[51] J. Wang, F. Yang, Preparation of 2-hydroxypropyl-β-cyclodextrin polymers crosslinked by poly(acrylic acid) for efficient removal of ibuprofen, Mater. Lett. 284 (2021), 128882, https://doi.org/10.1016/j.matlet.2020.128882.
[52] I. Krabicová, S.L. Appleton, M. Tannous, G. Hoti, F. Caldera, A.R. Pedrazzo, C. Cecone, R. Cavalli, F. Trotta, History of cyclodextrin nanosponges, Polymers 12 (2020) 1–23, https://doi.org/10.3390/POLYM12051122.
[53] G. Crini, S. Fourmentinn, E. Lichtfouse, Cyclodextrin Fundamentals, Reactivity and Analysis, 2018. http://www.springer.com/series/8380%0Ahttp://link.springer.com/10.1007/978-3-319-76159-6.
[54] A.P. Sherje, B.R. Dravyakar, D. Kadam, M. Jadhav, Cyclodextrin-based nanosponges: a critical review, Carbohydr. Polym. 173 (2017) 37–49, https://doi.org/10.1016/j.carbpol.2017.05.086.
[55] M. Miyauchi, A. Harada, Construction of supramolecular polymers with alternating α-, β-cyclodextrin units using conformational change induced by competitive guests, J. Am. Chem. Soc. 126 (2004) 11418–11419, https://doi.org/10.1021/ja046562q.
[56] W. Saenger, J. Jacob, K. Gessler, T. Steiner, D. Hoffmann, H. Sanbe, K. Koizumi, S.M. Smith, T. Takaha, Structures of the common cyclodextrins and their larger analogues - beyond the doughnut, Chem. Rev. 98 (1998) 1787–1802, https://doi.org/10.1021/cr9700181.
[57] T.J. Kim, B.C. Kim, H.S. Lee, Production of cyclodextrin using raw corn starch without a pretreatment, Enzym. Microb. Technol. 20 (1997) 506–509, https://doi.org/10.1016/S0141-0229(96)00186-X.
[58] H.J. Schneider, F. Hacket, V. Rüdiger, H. Ikeda, NMR studies of cyclodextrins and cyclodextrin complexes, Chem. Rev. 98 (1998) 1755–1785, https://doi.org/10.1021/cr970019t.
[59] S. Jia, D. Tang, J. Peng, Z. Sun, X. Yang, β-Cyclodextrin modified electrospinning fibers with good regeneration for efficient temperature-enhanced adsorption of crystal violet, Carbohydr. Polym. 208 (2019) 486–494, https://doi.org/10.1016/j.carbpol.2018.12.075.
[60] K. Hemine, A. Skwierawska, A. Kernstein, K. Kozłowska-Tylingo, Cyclodextrin polymers as efficient adsorbents for removing toxic non-biodegradable pimavanserin from pharmaceutical wastewaters, Chemosphere 250 (2020), https://doi.org/10.1016/j.chemosphere.2020.126250.
[61] M.A. Przybyla, G. Yilmaz, C. Remzi Becer, Natural cyclodextrins and their derivatives for polymer synthesis, Polym. Chem. 11 (2020) 7582–7602, https://doi.org/10.1039/d0py01464h.
[62] J. Rima, K. Assakera, β-Cyclodextrin polyurethanes copolymerized with beetroot fibers (Bio-Polymer) to clean-up water polluted by organics and spilled-oil, J. Petrol Environ. Biotechnol. (2018), https://doi.org/10.4172/2157-7463.1000368, 09.
[63] A.H. Karoyo, J. Yang, L.D. Wilson, Cyclodextrin-based polymer-supported bacterium for the adsorption and in-situ biodegradation of phenolic compounds, Front. Chem. 6 (2018), https://doi.org/10.3389/fchem.2018.00403.
[64] S. Brunauer, P.H. Emmett, E. Teller, Adsorption of gases in multimolecular layers, J. Am. Chem. Soc. 60 (1938) 309–319, https://doi.org/10.1021/ja01269a023.
[65] E.P. Barrett, L.G. Joyner, P.P. Halenda, The determination of pore volume and area distributions in porous substances. I. Computations from nitrogen isotherms, J. Am. Chem. Soc. 73 (1951) 373–380, https://doi.org/10.1021/ja01145a126.
[66] W.D. Harkins, G. Jura, Surfaces of solids. Xiii. A vapor adsorption of a monolayer area, and the areas occupied be nitrogen and other molecules on the surfase of a solid, J. Am. Chem. Soc. 66 (1944) 1366–1373.
[67] J. Kenvin, Characterization of Powders and Porous Materials with Pharmaceutical Excipinent Case Studies Theory of Adsorption Surface Area and Porosity Macro-Porosity Micro-porosity, 2008.
[68] A.M. Skwierawska, D. Nowacka, P. Nowicka, S. Rosa, K. Kozłowska-Tylingo, Structural adaptive, self-separating material for removing ibuprofen from waters and sewage, Materials 14 (2021) 1–23, https://doi.org/10.3390/ma14247697.
[69] M. Szőgyi, T. Cserháti, Chromatography of non-steroidal anti-inflammatory drugs: new achievements, Pharm. Anal. Acta (2012) 3–6, https://doi.org/10.4172/2153-2435.1000149, 03.
[70] A. Stafiej, K. Pyrzynska, F. Regan, Determination of anti-inflammatory drugs and estrogens in water by HPLC with UV detection, J. Separ. Sci. 30 (2007) 985–991, https://doi.org/10.1002/jssc.200600433.
[71] N.S. Mohamad Hanapi, M.M. Sanagi, A.K. Ismail, N. Saim, W.N.A. Wan Ibrahim, W.N.A. Wan Ibrahim, F. Mohd Marsin, Rapid determination of non-steroidal anti-inflammatory drugs in aquatic matrices by two-phase micro-electrodriven membrane extraction combined with liquid chromatography, J. Chromatogr. Sci. 56 (2018) 166–176, https://doi.org/10.1093/chromsci/bmx092.
[72] H. Speed, HPLC Non-steroidal Anti-inflammatory Drugs, (n.d.) 5–6.
[73] J.L. Santos, I. Aparicio, E. Alonso, M. Callejón, Simultaneous determination of pharmaceutically active compounds in wastewater samples by solid phase extraction and high-performance liquid chromatography with diode array and fluorescence detectors, Anal. Chim. Acta 550 (2005) 116–122, https://doi.org/10.1016/j.aca.2005.06.064.
[74] L. Ascar, I. Ahumada, A. López, F. Quintanilla, K. Leiva, Nonsteroidal anti-inflammatory drug determination in water samples by HPLC-DAD under isocratic conditions, J. Braz. Chem. Soc. 24 (2013) 1160–1166, https://doi.org/10.5935/0103-5053.20130150.
[75] Dantu krishna, Murali, European Patent Application, EP Patent 0879946A2. 1, 2012, pp. 1–14. http://info.sipcc.net/files/patent/fulltext/EP/200605/EP2099194A1/EP2099194A1.PDF.
[76] M. Ahmed, F. Azam, A. Gbaj, A.E. Zetrini, A.S. Abodlal, A. Rghigh, E. Elmahdi, A. Hamza, M. Salama, S.M. Bensaber, Ester prodrugs of ketoprofen: synthesis, in vitro stability, in vivo biological evaluation and in silico comparative docking studies against COX-1 and COX-2, Curr. Drug Discov. Technol. 13 (2016) 41–57, https://doi.org/10.2174/1570163813666160119092807.
[77] Y.H. Yao, X.J. Zou, Y. Wang, H.Y. Yang, Z.H. Ren, Z.H. Guan, Palladium-catalyzed asymmetric markovnikov hydroxycarbonylation and hydroalkoxycarbonylation of vinyl arenes: synthesis of 2-arylpropanoic acids, Angew. Chem. Int. Ed. 60 (2021) 23117–23122, https://doi.org/10.1002/anie.202107856.
[78] C. Ramminger, D. Zim, V.R. Lando, V. Fassina, A.L. Monteiro, Transition-metal catalyzed synthesis of ketoprofen, J. Braz. Chem. Soc. 11 (2000) 105–111, https://doi.org/10.1590/S0103-50532000000200002.
[79] H. Neumann, A. Brennführer, M. Beller, An efficient and practical sequential one-pot synthesis of suprofen, ketoprofen and other 2-arylpropionic acids, Adv. Synth. Catal. 350 (2008) 2437–2442, https://doi.org/10.1002/adsc.200800415.
[80] A.L. Ong, A.H. Kamaruddin, S. Bhatia, Current technologies for the production of (S)-ketoprofen: process perspective, Proc. Biochem. 40 (2005) 3526–3535, https://doi.org/10.1016/j.procbio.2005.03.054.
[81] Honeywell International Inc, European Patent Application, EP Patent 0879946A2. 1, 2007, pp. 1–14. http://info.sipcc.net/files/patent/fulltext/EP/200605/EP2099194A1/EP2099194A1.PDF.
[82] P.E.P. Garvin, United States Patent, vol. 19, 1989, p. 934.
[83] A. Labidi, Diclofenac Synthesis, vol. 3, Royal Society of Chemistry, 2021, pp. 3–5, https://doi.org/10.17605/OSF.IO/F9XWS.
[84] D. Oak, C. Christi, L. Brad, G.N. Mott, E.G. Zey, C. Christi, L. Gary, United States Patent, vol. 19, 1991.
[85] N.A. Samah, M.J. Sánchez-Martín, R.M. Sebastián, M. Valiente, M. López-Mesas, Molecularly imprinted polymer for the removal of diclofenac from water: synthesis and characterization, Sci. Total Environ. 631–632 (2018) 1534–1543, https://doi.org/10.1016/j.scitotenv.2018.03.087.
[86] I.M. Jauris, C.F. Matos, C. Saucier, E.C. Lima, A.J.G. Zarbin, S.B. Fagan, F.M. Machado, I. Zanella, Adsorption of sodium diclofenac on graphene: a combined experimental and theoretical study, Phys. Chem. Chem. Phys. 18 (2016) 1526–1536, https://doi.org/10.1039/c5cp05940b.

[87] Z.A. ALOthman, A.Y. Badjah, O.M.L. Alharbi, I. Ali, Synthesis of chitosan composite iron nanoparticles for removal of diclofenac sodium drug residue in water, Int. J. Biol. Macromol. 159 (2020) 870–876, https://doi.org/10.1016/j.ijbiomac.2020.05.154.
[88] M. El-Kemary, S. Sobhy, S. El-Daly, A. Abdel-Shafi, Inclusion of Paracetamol into β-cyclodextrin nanocavities in solution and in the solid state, Spectrochim. Acta Mol. Biomol. Spectrosc. 79 (2011), https://doi.org/10.1016/j.saa.2011.05.084, 1904–1908.
[89] S. Talegaonkar, Development and characterization of paracetamol complexes with hydroxypropyl-ß-cyclodextrin, Iran. J. Pharm. Res. (IJPR) 6 (2007) 95–99, https://doi.org/10.22037/ijpr.2010.705.
[90] M. Herrmann, O. Olsson, R. Fiehn, M. Herrel, K. Kümmerer, The significance of different health institutions and their respective contributions of active pharmaceutical ingredients to wastewater, Environ. Int. 85 (2015) 61–76, https://doi.org/10.1016/j.envint.2015.07.020.
[91] N.J.D.G. Reyes, F.K.F. Geronimo, K.A. V Yano, H.B. Guerra, L. Kim, Matrices : Occurrence , Pathways , and Treatment Processes, 2021.
[92] K.H. Langford, K.V. Thomas, Determination of pharmaceutical compounds in hospital effluents and their contribution to wastewater treatment works, Environ. Int. 35 (2009) 766–770, https://doi.org/10.1016/j.envint.2009.02.007.
[93] R.L. Oulton, T. Kohn, D.M. Cwiertny, Pharmaceuticals and personal care products in effluent matrices: a survey of transformation and removal during wastewater treatment and implications for wastewater management, J. Environ. Monit. 12 (2010), https://doi.org/10.1039/c0em00068j, 1956–1978.
[94] M.E.M. Ali, A.M. Abd El-Aty, M.I. Badawy, R.K. Ali, Removal of pharmaceutical pollutants from synthetic wastewater using chemically modified biomass of green alga Scenedesmus obliquus, Ecotoxicol. Environ. Saf. 151 (2018) 144–152, https://doi.org/10.1016/j.ecoenv.2018.01.012.
[95] M. Usman, A. Ahmed, B. Yu, S. Wang, Y. Shen, H. Cong, Simultaneous adsorption of heavy metals and organic dyes by β-Cyclodextrin-Chitosan based cross-linked adsorbent, Carbohydr. Polym. (2021) 255, https://doi.org/10.1016/j.carbpol.2020.117486.
[96] T. Thiebault, M. Boussafir, L. Fougère, E. Destandau, L. Monnin, C. Le Milbeau, Clay minerals for the removal of pharmaceuticals: initial investigations of their adsorption properties in real wastewater effluents, Environ. Nanotechnol. Monit. Manag. 12 (2019), https://doi.org/10.1016/j.enmm.2019.100266.
[97] I.A. Lawal, M.M. Lawal, S.O. Akpotu, M.A. Azeez, P. Ndungu, B. Moodley, Theoretical and experimental adsorption studies of sulfamethoxazole and ketoprofen on synthesized ionic liquids modified CNTs, Ecotoxicol. Environ. Saf. 161 (2018) 542–552, https://doi.org/10.1016/j.ecoenv.2018.06.019.
[98] A.F.M. Streit, G.C. Collazzo, S.P. Druzian, R.S. Verdi, E.L. Foletto, L.F.S. Oliveira, G.L. Dotto, Adsorption of ibuprofen, ketoprofen, and paracetamol onto activated carbon prepared from effluent treatment plant sludge of the beverage industry, Chemosphere (2021) 262, https://doi.org/10.1016/j.chemosphere.2020.128322.
[99] L. Sellaoui, L.F.O. Silva, M. Badawi, J. Ali, N. Favarin, G.L. Dotto, A. Erto, Z. Chen, Adsorption of ketoprofen and 2- nitrophenol on activated carbon prepared from winery wastes: a combined experimental and theoretical study, J. Mol. Liq. 333 (2021), 115906, https://doi.org/10.1016/j.molliq.2021.115906.
[100] G. Peng, M. Zhang, S. Deng, D. Shan, Q. He, G. Yu, Adsorption and catalytic oxidation of pharmaceuticals by nitrogen-doped reduced graphene oxide/Fe3O4 nanocomposite, Chem. Eng. J. 341 (2018) 361–370, https://doi.org/10.1016/j.cej.2018.02.064.
[101] C.P. Bergmann, F.M. Machado, Carbon nanomaterials as adsorbents for environmental and biological applications. https://doi.org/10.1007/978-3-319-18875-1, 2015.
[102] E.C. Lima, A. Hosseini-Bandegharaei, J.C. Moreno-Piraján, I. Anastopoulos, A critical review of the estimation of the thermodynamic parameters on adsorption equilibria. Wrong use of equilibrium constant in the Van't Hoof equation for calculation of thermodynamic parameters of adsorption, J. Mol. Liq. 273 (2019) 425–434, https://doi.org/10.1016/j.molliq.2018.10.048.
[103] F. Haghseresht, G.Q. Lu, Adsorption characteristics of phenolic compounds onto coal-reject-derived adsorbents, Energy Fuel. 12 (1998) 1100–1107, https://doi.org/10.1021/ef9801165.
[104] W.J. Weber, J.C. Morris, in: Advances in Water Pollution Research BT - Proc. Int. Conf. On Water Pollution Symp., Pergamon Press, Oxford, London, 1962. Publ. Div.
[105] S. Heydari, R.M. kakhki, Thermodynamic study of complex formation of β-cyclodextrin with ibuprofen by conductometric method and determination of ibuprofen in pharmaceutical drugs, Arab. J. Chem. 10 (2017) S1223–S1226, https://doi.org/10.1016/j.arabjc.2013.02.021.
[106] P. Mura, G.P. Bettinetti, A. Manderioli, M.T. Faucci, G. Bramanti, M. Sorrenti, Interactions of ketoprofen and ibuprofen with β-cyclodextrins in solution and in the solid state, Int. J. Pharm. 166 (1998) 189–203, https://doi.org/10.1016/S0378-5173(98)00035-0.
[107] S. Das, U. Subuddhi, Studies on the complexation of diclofenac sodium with β-cyclodextrin: influence of method of preparation, J. Mol. Struct. 1099 (2015) 482–489, https://doi.org/10.1016/j.molstruc.2015.07.001.
[108] S. Zidane, A. Maiza, H. Bouleghlem, B. Fenet, Y. Chevalier, Inclusion complex of Tramadol in β-cyclodextrin enhances fluorescence by preventing self-quenching, J. Inclusion Phenom. Macrocycl. Chem. 93 (2019) 253–264, https://doi.org/10.1007/s10847-018-0874-1.